A Barotropic Model for Operational Prediction of Tracks of Tropical Storms

FREDERICK SANDERS[1]

Massachusetts Institute of Technology, Cambridge

ARTHUR C. PIKE

National Hurricane Center, NOAA, Coral Gables, Fla.

JOHN P. GAERTNER

Massachusetts Institute of Technology, Cambridge

(Manuscript received 13 May 1974, in revised form 17 December 1974)

ABSTRACT

In response to early success in barotropic prediction of selected storm tracks, we undertook development of a system for operational application. The main effort was in devising a statistical method for automated analysis of the flow averaged in depth from 1000 to 100 mb. Initially the storm was represented in the flow pattern in a parametric way. Numerical calculation was carried out over a grid area from the Equator to 55°N latitude and from 36.5° to 123.5°W longitude, with a mesh length of 154 km. It was necessary to modify the prediction equation to prevent spurious retrogression of the long waves, despite the restricted grid area. It was also necessary to employ truncation-error control in the evaluation of Jacobians to avoid a spuriously slow predicted speed for the tropical storm, despite the small mesh length.

The method of representing the storm in the initial flow pattern was found unsatisfactory. After considerable experimentation, we now require the pattern of the initial streamfunction over the region of storm influence to represent exactly the sum of a steering flow, derived from the best concurrent estimate of storm motion, and an idealized vortex described in terms of three variable parameters.

The present model appears to have modest skill with respect to persistence and climatology in forecasts for the ranges from 24 to 72 h. Prominent present sources of error in barotropic forecasting are discussed, with recommendation for their mitigation, suggesting an achievable accuracy of 75 n mi at 24 h and 300 n mi at 72 h. Further reduction of errors would require baroclinic models.

1. Introduction

Experimental barotropic predictions described by Sanders and Burpee (1968) confirmed the traditional view (e.g., Bowie, 1922; Jordan, 1952) that the track of a tropical storm can be described to a first approximation as the effect of "steering" of the cyclonic vortex by the large-scale environmental current within which it is embedded. We were thus encouraged to devise a model for operational use at the National Hurricane Center at Miami. This paper describes the development of the so-called SANBAR model, our experiences with its use, and our views of prospects for future improvements in the accuracy of track forecasts. A preliminary report has been given elsewhere (Sanders, 1970).

2. Automated analysis

An adequate automated analysis of the initial tropospheric wind field was a crucial necessity. For reasons given in the earlier cited works, we require the wind averaged through the depth of the layer from 1000 to 100 mb and cannot rely on the height data except, indirectly, poleward of about 30° latitude. We chose to use Eddy's (1967) statistical technique, a method in which values of the element to be analyzed are given by a set of multiple regression equations with each grid-point value as a predictand, and the observed values at appropriate nearby locations as predictors. The technique closely resembles Gandin's (1963) method of "optimum interpolation."

Our analysis treats separately the zonal and meridional components of the wind, or more specifically the departure of these components from the respective latitudinal band means. The band means are obtained from the available observations for a particular synoptic time. To calculate the regression equations we need the correlation between simultaneously observed pairs of observations as a function of separation distance between the observation locations. We did not follow Eddy's procedure of calculating this function for an individual synoptic time because we felt

[1] Much of the work was done while the senior author was on sabbatical leave at the National Hurricane Research Laboratory.

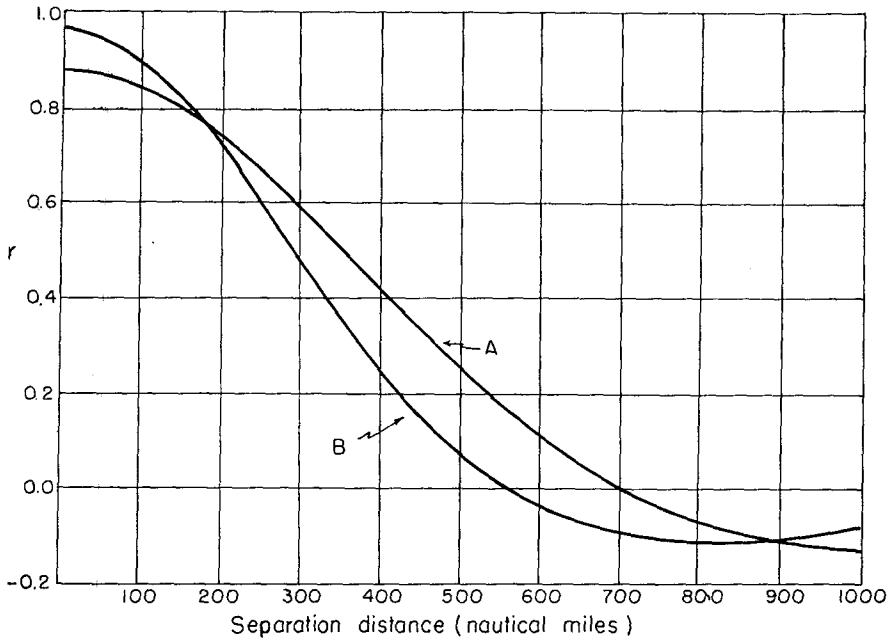

FIG. 1. Correlation as a function of separation distance, for departures of vertically-averaged wind from synoptic zonal average value. Curves designated A are derived from a data sample of 1799 soundings on selected hurricane days in September 1960, September 1961, October 1963, September 1965, October 1966 and October 1967. Curves designated B are derived from a sample of 1713 soundings from 6–13 September 1971.

that the number of available observations was too small to yield a reliable result, and because the computing expense would have been considerable in operational practice. Rather, we derived the function for a sample of observations covering a substantial period of time and a substantial area (the Gulf of Mexico, the Caribbean Sea, the western and central North Atlantic Ocean, North America, and the eastern Pacific Ocean). Thus we assumed, in effect, that the statistics of the wind were homogeneous and stationary; and since we took no account of the orientation of the line connecting the observation locations, we further assumed isotropy.

Correlation functions for the zonal and meridional wind components derived from two sets of data are shown in Fig. 1. In both instances, the raw correlations given by the data sets have been smoothed and the curves have been extended parabolically to zero from the smallest separation distance at which the slope could be reliably calculated. The two pairs of curves differ only slightly, reflecting small differences in the spectral characteristics of the data during the two collection periods. Though we have made no systematic comparison of forecasts based on the two curves, our impression based on limited experience is that the difference in tracks is smaller than differences arising from a number of other sources, which will be discussed later. Both data sets were carefully pruned by correction of spurious observations where possible or by elimination where not. When the results are then applied to the operational environment, the correlations are not strictly appropriate since less care is taken in real time. We would prefer, however, to accept inconsistency rather than sloth.

The grid area for analysis extends from the Equator to 55°N latitude and from 36.5° to 123.5°W longitude, on a Mercator projection. The grid mesh length is 154 km at the standard parallel of 22.5°N latitude.

The regression equation for each grid point is obtained by considering all stations within a distance equal to the zero-correlation distance given by the function shown in Fig. 1 (560 to 800 n mi, depending on the element and data sample). Stepwise screening regression, based upon the correlation coefficients appropriate to distances from station to grid point and between stations, yields a multiple linear regression equation. Stations are added individually until the marginal increase in explained variance is less than 0.1%. Sample equations for the zonal components are illustrated in Fig. 2. Grid point A is not particularly close to any observation location. Consequently, it relies about equally on the observations at several stations a moderate distance away and the result is relatively uncertain. In contrast, grid point B is very close to an observing station, so that it relies almost exclusively on a single observation and yields a relatively certain result.

Since the oceanic portions of the grid are almost entirely devoid of rawinsonde observations, the analysis is aided by the manual provision of bogus wind ob-

servations at a fixed set of 44 points at prescribed geographic positions. See Williams (1972) for a listing of the coordinates of these points. These observations have been obtained from a variety of sources, ranging from sheer imagination, through 12 h prognostic height fields, jet aircraft, and surface ship observations, to ATS III cloud-motion vectors. The bogus data are treated in the derivation of regression equations as though they were genuine wind observations.

Our statistical analysis procedure has both advantages and disadvantages relative to the more conventional objective analysis techniques. First, it has the virtue of a rationale to guide the choice of weighting factors to be assigned to observations (though pragmatism would require us to concede that rationalism becomes a virtue only when it results in demonstrably better forecasts). Second, it relies little on a "first guess" (the synoptic zonal average value in effect fulfills this role), and therefore does not suffer in circumstances when conventional first guesses are poor. Finally, the residual unexplained variance, which is a by-product of the computation of regression equations, is a quantitative measure of our ignorance associated with a given station network.

On the other hand, our analysis technique is not well suited to the availability of "observations of opportunity." The addition of a single sounding at a location not on our regular list requires the recalculation of scores of regression equations. The loss of a single station on our list produces a like consequence. We have found the time and expense of this added computation operationally unacceptable. We thus ignore, for example, the occasional wind sounding from a ship elsewhere but on one of the Ocean Stations, hoping that it will improve the reliability of the bogus data in its vicinity. To mitigate the consequences of missing data for a regular station, we have provided regression equations, similar to the grid-point equations, which estimate a value for the station from the values at surrounding stations. Generally, we have not made effective systematic use of observational material from locations which are variable from day to day. Much of the data over oceanic regions of the globe is of that character and will doubtless continue to be so.

3. Representation of the tropical storm

The representation of the tropical storm in the wind analysis is a difficult matter. The difficulty arises because the tropical storm is a rare event and because its wind structure is badly observed. For reasons de-

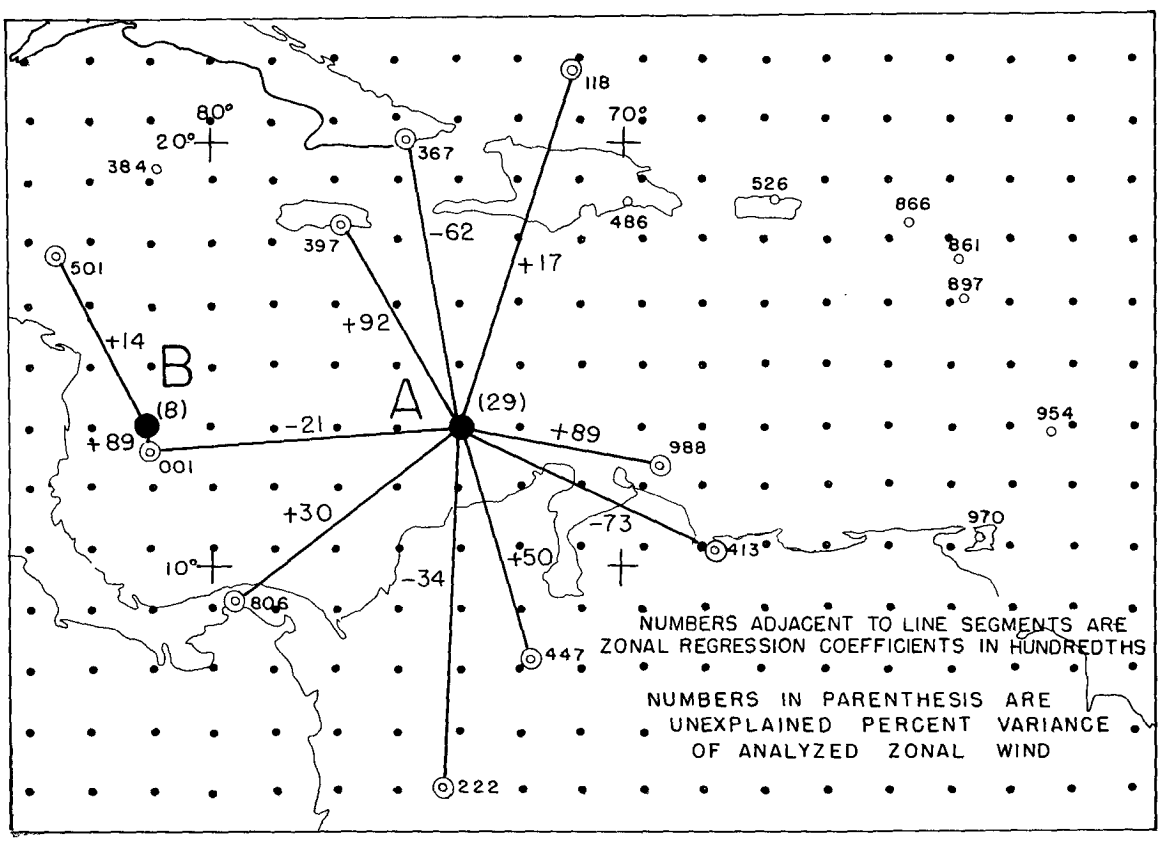

FIG. 2. Portion of the analysis grid with sample regression equations shown schematically.

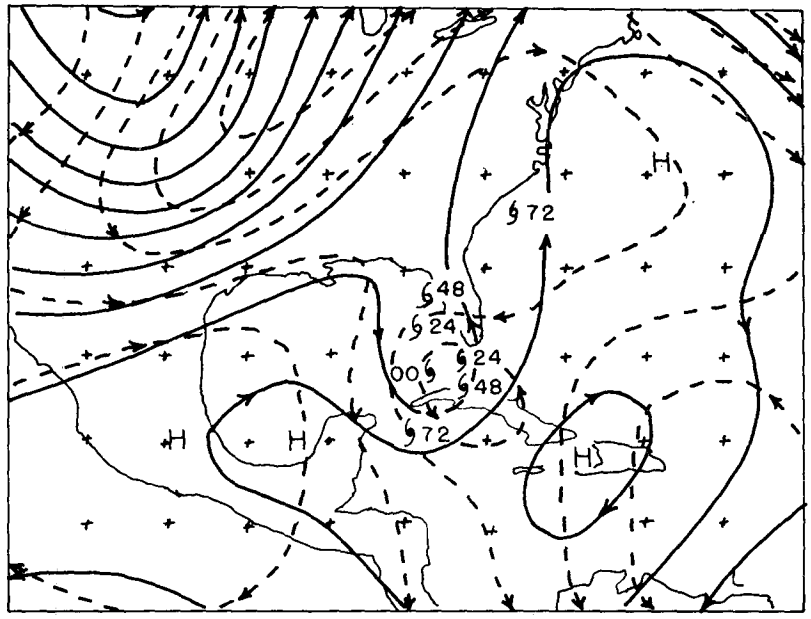

FIG. 3. Initial (solid) streamfunction for 0000 GMT 17 October 1968, and 48 h prognostic (dashed) pattern. The line interval is 3×10^6 m^2 s^{-1}. The initial and forecast positions of Gladys are shown by hurricane symbols with filled centers, labelled with the appropriate number of hours after the initial time. Corresponding observed positions of the storm are shown by hurricane symbols with open centers. Only a portion of the forecast area is shown.

scribed in the works cited in the Introduction, we must represent the storm in some reasonable way in our initial analysis. The statistical analysis scheme, left to itself, would fail to detect the presence of the storm, unless one or more rawinsonde observations fell within its circulation. If the observation were strongly affected by the storm, the analysis program would regard it as erroneous, like any other observation sufficiently removed from the climatic mean, and would discard it.

Our initial attempt to deal with this problem, described in detail by Sanders (1970), was to regard the storm circulation as an axisymmetric vortex of purely tangential motion, the profile of which was specified by the maximum wind, the distance from the center to the ring of maximum wind (usually taken as 20 n mi), and the distance from the center to the radius at which no influence was felt (which averages about 300 n mi). These storm parameters, plus the location of the center, were specified from the surface analysis and the most recent aircraft reconnaissance or other information. If a rawinsonde observation lay within the maximum influence distance, a storm-wind vector was subtracted from it, having a direction and speed appropriate to the bearing and distance of the station from the storm center. The residual wind was then regarded as a measure of the large-scale environmental pattern and was used in the statistical analysis. Upon completion of this analysis, an appropriate storm-wind vector was added to all grid-point values within the maximum influence distance. In preliminary tests the residual winds appeared to be quite reasonable, and the implicit steering yielded forecast storm tracks which were in good accord with those observed. Subsequent operational and research experience, however, revealed that our optimism was ill-founded; further attempts to deal with the problem will be discussed later.

4. Initial operational forecasts

The first real-time operational forecasts, for Hurricane Gladys 1968, served mainly to disclose a large-scale problem which had not arisen in any of a substantial number of test predictions: spurious retrogression of the long-wave components of the flow pattern. An example is shown in Fig. 3. The predicted storm reverses direction after the first 24 h, heading southwestward at an accelerating pace, while the actual hurricane merely slows during the second 24 h period and then accelerates toward the northeast.

The forecast failure was due to the unrealistic development of northerly steering-wind components over the central portion of the map area. Despite the constancy of streamfunction values on the boundaries of a grid covering slightly less than one-quarter of the hemisphere, a substantial error pattern in streamfunction with zonal hemispheric wavenumber 4 had developed by 48 h. The presence in the initial data of a ridge and trough extending over virtually

the entire meridional extent of the grid was probably responsible for this forecast failure. As an immediate palliative (which we have not since replaced), we resorted to the usual high-latitude practice (e.g., Cressman, 1958) of altering the prediction equation by the addition of a term which, in structure, can be argued to simulate the effect of mean divergence over the layer from 1000 to 100 mb. The value of this term required to prevent the development of the characteristic error pattern, however, implied a mean divergence much larger than could be reasonably expected. Therefore, it is not clear what physical process we are simulating with this empirical device. Its effect, however, is to prevent rapid movement of the longer wavelengths, but without significant effect on the shorter wavelengths. A revised forecast is shown in Fig. 4. It is clear that the large-scale flow pattern changes in a much more modest way, though the initial ridge in the western Atlantic and central Caribbean still moves westward; and the forecast is qualitatively realistic. Still, we can hardly be satisfied with the present remedy. Aside from the intellectual discomfort pointed out above, there is the practical consideration that cases of erratic tracks may be damaged by our long-wave control mechanism, since they may represent instances in which substantial changes do in fact occur in the larger scales of motion.

5. MODified SANBAR

Despite the relative paucity of tropical storms within reach of the rawinsonde network during the ensuing years, it was clear by the end of the 1971 hurricane season that in the early portions of SANBAR forecasts, whether made in the operational environment (Pike, 1972) or under research conditions (Williams, 1972; Gaertner, 1973), large but erratic direction errors occurred, and forecast track speeds were systematically slow by an average of about 25%. These flaws notwithstanding, the SANBAR forecasts were at least as accurate as other guidance forecasts in the range from 48 to 72 h (Pike, 1972).

The difficulty seemed to lie in the initial wind field in the region of influence of the tropical storm. Williams (1972), for example, showed instances in which the residual wind in a rawinsonde observation, after subtraction of a vortex contribution as described above, was palpably unrealistic, even to the point of being directly opposite to the concurrent track direction. Evidently, vortex structure is so variable that even our fairly elaborate attempt to parameterize it is unable to separate reliably the basic current from the storm circulation.

Pike (1972) dealt with this situation by discarding entirely any rawinsonde observation within the maximum influence distance of the storm and substituting for it the vector sum of the best available estimate of the concurrent track velocity plus the appropriate contribution from the idealized axisymmetric storm vortex. This wind then was used in the analysis at relevant grid points outside the region of storm influence. Moreover, a wind of this type was calculated for each grid point within the influenced region, which was thus excluded from the statistical analysis. Then the vorticity and streamfunction initialization and the forecast calculation proceded as before. Applying this modified (MOD) SANBAR model to a sample of 24

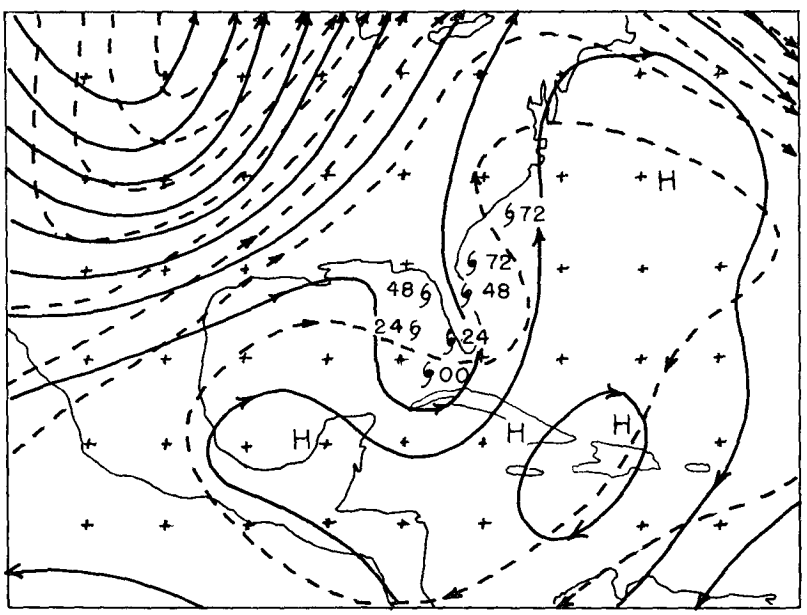

FIG. 4. As in Fig. 3 except that the forecast is calculated with the long-wave control. See text.

storm forecasts during the 1971 season, Pike found much improved correspondance between forecast and observed direction during the first 24 h and substantially reduced position errors at all times out to the maximum range of 72 h. The speed bias, however, was only slightly reduced.

6. FAST SANBAR

Gaertner (1973) experimented with a set of 28 storm forecasts from the 1971 season, including 11 in common with Pike's sample. Working at MIT with a slightly different set of regression equations for analysis and with independently derived bogus data and storm parameters, Gaertner found relatively small directional errors in forecasts made with either the original or the modified model. In further contrast with Pike's result, Gaertner's MOD SANBAR forecasts removed about a third of the slow bias in forecasts made with the original model but the two sets of 24 h results from the modified model shared a common residual slow bias of about 20% of the actual displacement.

In the subsequent search for causes of the slow bias, two possibilities were considered and discarded, while two others provided a viable solution.

First, we considered that the long-wave control might also be spuriously retarding the speed of the tropical storm. For a rough estimate we assumed the simple one-dimensional wave in the streamfunction field given by

$$\psi(x,t)=\psi_0 \sin\frac{2\pi}{L}(x-ct). \tag{1}$$

If the physical situation is expressed simply as conservation of relative vorticity, then

$$\frac{\partial\zeta}{\partial t}=-U\frac{\partial\zeta}{\partial x},$$

or

$$\nabla^2\frac{\partial\psi}{\partial t}=-U\frac{\partial^3\psi}{\partial x^3}, \tag{2}$$

where U is a constant speed. For this situation it is immediately obvious that c, the phase speed of the wave, is identical to U, the speed of the advecting wind. The prediction equation containing the long-wave control, however, has the form

$$(\nabla^2-H)\frac{\partial\psi}{\partial t}=-U\frac{\partial\zeta}{\partial x}, \tag{3}$$

where H is a constant. In this case the phase speed is given by

$$C=U/(1+HL^2/4\pi^2). \tag{4}$$

Since, for the value of H used in the SANBAR calculations, the phase speed corresponding to a wavelength around 300 nm is about $0.99U$, and since the addition of the control had a virtually imperceptible effect on the storm speed in the early portions of the Gladys forecasts (among others), this effect was found innocent.

Second, we considered that an equivalent-barotropic effect might be present in tropical wind data after all, and that a wind speed stronger than the tropospheric mean might be appropriately used. Accordingly, we examined the 1971 data sample used to establish the correlation function shown in Fig. 1. The fundamental modeling approximation is

$$\mathbf{V}(x,y,p,t)=A(p)\bar{\mathbf{V}}(x,y,t). \tag{5}$$

Since we had computed for other purposes the means in the lower and upper halves of the layer from 1000 to 100 mb for each sounding, it was convenient to define the equivalent-barotropic factor $\overline{A^2}$ as

$$\overline{A^2}\equiv\frac{1}{2}\left[\left(\frac{\bar{\mathbf{V}}^L\cdot\bar{\mathbf{V}}}{\bar{V}}\right)^2+\left(\frac{\bar{\mathbf{V}}^U\cdot\bar{\mathbf{V}}}{\bar{V}}\right)^2\right], \tag{6}$$

where $\bar{\mathbf{V}}^L$ and $\bar{\mathbf{V}}^U$ are the mean winds in the layer from 1000 to 550 mb, and from 550 to 100 mb, respectively. That is, we took account only of the component of wind in the direction of the mean wind and we neglected the effect of systematic wind variation within each half. Values of $\overline{A^2}$ varied considerably from sounding to sounding, but a median value for winds of moderate strength was about 1.07. Thus, though a 7% enhancement of the mean winds on which the SANBAR model relies might be justified, the modification would not be enough to account for a major portion of the slow bias. Moreover, with the MOD SANBAR variation, an appropriate enhancement factor is implicitly included in the steering wind forced into the initial analysis. Finally, some test forecasts made with enhanced input wind speed exacerbated a tendency for spurious growth of area-average kinetic energy during the forecast period, to the detriment of the 48 and 72 h forecasts of storm position. Consequently, we decided to shelve the introduction of an equivalent-barotropic effect until the question of kinetic-energy growth, arising from necessarily assumed lateral boundary condition, was dealt with.[2]

[2] An empirical stabilization of the model's total kinetic energy K has been introduced by Pike. Since

$$K=\frac{1}{2}\int\left[\left(\frac{\partial\psi}{\partial x}\right)^2+\left(\frac{\partial\psi}{\partial y}\right)^2\right]dA,$$

where dA is an element of area, the computed streamfunction at time t may be modified by

$$\psi_t(\text{modified})=\psi_t\left(\frac{K_0}{K_t}\right)^{\frac{1}{2}}$$

at each time step so the $K_t(\text{modified})=K_0$. This procedure causes no apparent deterioration in the forecast accuracy and prevents the computational instability that has occasionally occurred.

Next, we considered the effects of truncation error. The hurricane obviously has considerable power in wavelengths which are not large relative to even our small mesh length. Again we dealt with the simple field of streamfunction given by (1) and the prediction equation given by (2). Though the true value of the phase speed c is the advecting wind speed U, the solution of the simple centered finite-difference analogue yields a phase speed c', given by (Phillips, 1972)

$$c' = L \sin^{-1}\left[\frac{U\Delta t}{\Delta x}\sin\left(\frac{2\pi}{L}\Delta x\right)\right] \Big/ (2\pi\Delta t). \qquad (7)$$

For our case, $\Delta t = 30$ min, $\Delta x = 154$ km, and U is taken as 10 m s^{-1}. Then the ratio of the finite-difference speed to the true speed is as shown in Fig. 5. Since the effective wavelength might be taken as twice the typical maximum influence distance of a tropical storm, or about seven mesh lengths, a truncation error of about 12% might be anticipated. Accordingly, the forecast program was modified to include the truncation-error control described by Shuman and Vanderman (1968). In a sample of 16 of his 28 cases, Gaertner made a revised MOD SANBAR forecast with the Shuman-Vanderman control. The forecasts with this device yielded initial 12 h displacements which averaged 16% smaller than the prescribed initial steering speeds, whereas the corresponding displacements in the earlier 74 forecasts were 28% smaller than the prescribed steering. Therefore, there was good agreement with theoretical expectations and a substantial amount of the slow bias had been removed.

In view of the substantial amount of remaining bias, it seemed that the strength of the steering flow, as given by the initial streamfunction pattern, must be too weak. This strength is given simply by $\Delta\psi/2R$, where $\Delta\psi$ is the difference of streamfunction at the two ends of a line segment normal to the prescribed direction of the storm, centered on the storm and extending to the maximum influence radius R. This speed, for Gaertner's sample of 16 storms, averaged 14% less than the prescribed steering speed, accounting for nearly all of the remaining bias. Evidently, the relaxation procedure for obtaining the initial streamfunction from the calculated vorticity, though apparently converging satisfactorily, was systematically failing to reproduce the correct steering speeds in the vicinity of the storm. Elsewhere in the grid area, however, agreement was good. This difficulty had not arisen in the earlier forecasts based on manual analysis.

Limited study of the individual cases suggested that the discrepancy arose principally for storms far from the reach of rawinsonde data. We believe that uncertainty in the assignment of bogus winds and lack of information in the statistical analysis both lead to underestimates of the wind speed in regions of sparse information. In the extreme, for example, absolute lack of knowledge of any kind would dictate zero as a most probable estimate. Therefore, the area influenced by the storm is generally embedded in a region of analyzed flow weaker than the prescribed steering speed. Since the relaxation has the characteristics of a smoothing operation, the steering winds in the storm area are contaminated by the weaker ones outside during the relaxation process.

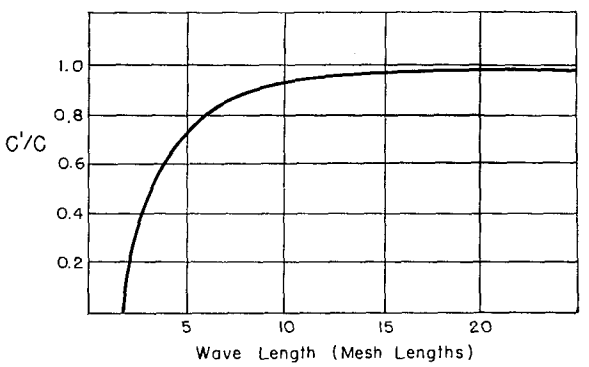

FIG. 5. Ratio of finite-difference speed to true phase speed as a function of wavelength, in mesh lengths, for $\Delta x = 154$ km, $\Delta t = 30$ min, $U = 10$ m s^{-1}.

To confirm culpability and to provide a remedy, we adopted a straightforward method of dealing with this last source of error. We decided simply to pre-calculate the fields of streamfunction and vorticity from the storm parameters and the steering velocity at all grid points within the area influenced by the storm. We do not require, however, that the streamfunction values at the internal grid points remain constant, only that they all change simultaneously by the same amount during the iteration process.

We may have overspecified the problem, and cannot prove that our procedure converges, but it has given us no trouble to date, despite large residuals and visible raggedness in the relaxed values at grid points immediately outside the influence region. This method of calculating the vorticity from the analytical storm vortex discounts any contribution from the relative vorticity of the steering flow. This vorticity is utterly small compared to the enormous values calculated from the analytical expression. The extraordinarily large values at the grid points closest to the center are immediately reduced by truncation error during the forecast calculation, evidently with no detrimental effect upon the forecast track.

Gaertner's 16 revised forecasts, based on this FAST SANBAR model, showed a residual slow bias in the initial 12 h displacement of only 3.5%. Since the standard deviation was about 10%, this remaining bias has little statistical significance. In Gaertner's method of error measurement, moreover, the observed displacement is compared with the projection of the forecast displacement upon it, so that a forecast with the correct speed but an inaccurate direction would

TABLE 1. 1973 FAST SANBAR position errors (n mi).

Storm	Date	Initial Time (GMT)	Initial Latitude (°N)	Initial Longitude (°W)	Time range 0 hours	24 hours	48 hours	72 hours
Alice	03	00	28	65	0	115	230	595
(July)	03	12	30	65	5	20	140	540
	04	00	32	65	25	70	235	—
	04	12	33	65	20	50	240	—
								(Extratropical)
	05	00	35	65	15	60	—	—
	05	12	37	64	5	180	—	—
Mean					12	82	211	568
Brenda	19	00	21	87	5	100	240	375
(August)	19	12	21	88	0	70	205	—
	20	00	21	90	10	100	215	—
								(Inland)
	20	12	20	92	10	135	—	—
Mean					6	101	220	375
Christine	31	00	10	46	85	180	250	315
(August–September)	31	12	12	46	25	140	130	145
	01	00	13	49	20	50	250	—
	01	12	14	52	25	145	305	—
								(Weakened)
	02	00	15	54	25	70	—	—
	02	12	16	57	20	40	—	—
Mean					33	104	222	230
Delia	03	00	24	88	5	170	220	50
(September)	03	12	25	90	65	95	215	150
	04	00	28	92	30	150	440	—
	04	12	28	94	35	325	425	—
								(Inland)
	05	00	29	95	10	220	—	—
	05	12	28	96	30	60	—	—
Mean					29	170	325	100
Ellen	19	00	27	47	0	15	215	580
(September)	19	12	28	50	20	160	380	1005
	20	00	28	53	40	320	670	—
	20	12	30	54	10	95	365	—
								(Extratropical)
	21	00	32	54	20	15	—	—
	21	12	34	54	25	35	—	—
Mean					19	107	408	792
Fran	10	00	32	55	0	130	*	*
(October)								
Gilda	18	00	20	80	0	40	125	255
(October)	18	12	20	80	35	85	25	405
	19	00	22	79	0	120	330	1045
	19	12	23	78	10	100	160	820
	20	00	24	77	25	130	500	—
	20	12	24	76	5	115	410	—
								(Extratropical)
	21	00	25	76	10	120	—	—
	21	12	26	76	20	65	—	—
Mean					13	94	258	631
All storms								
Mean					19	111	275	483
Median					15	100	235	405

* Fetched up smartly against eastern boundary of grid.

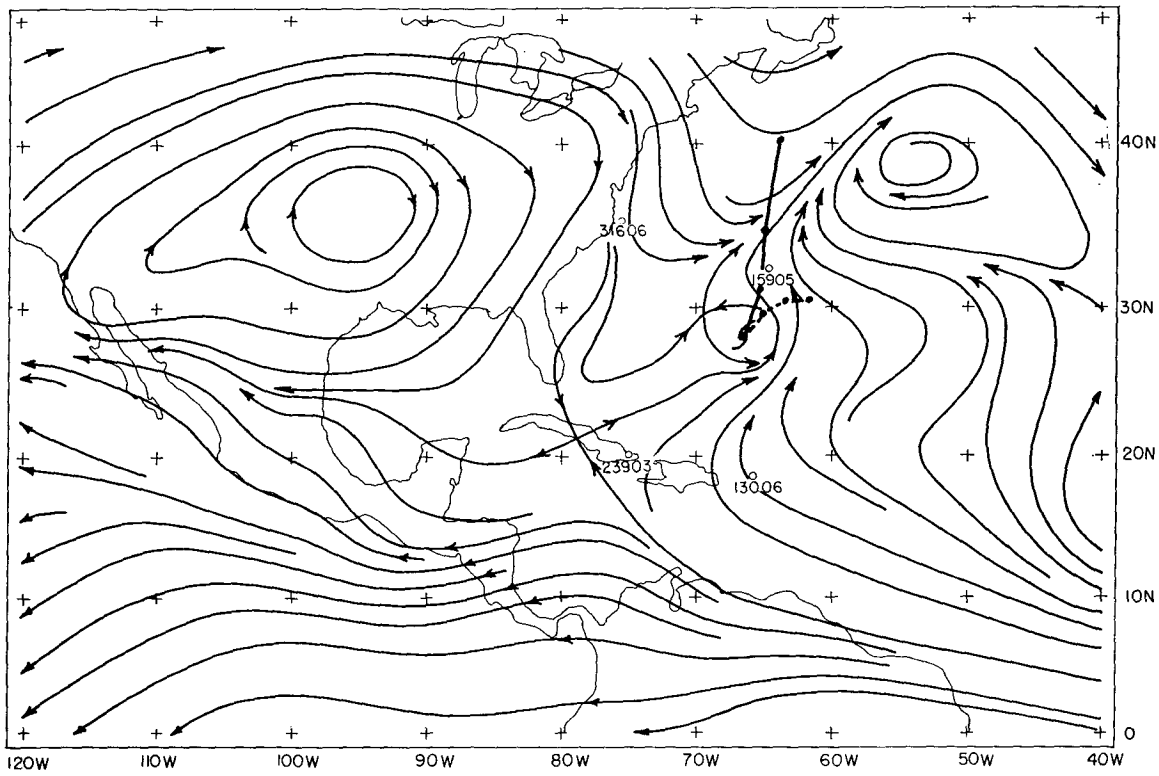

FIG. 6. Initial flow pattern at 0000 GMT 3 July 1973, with subsequent observed track of Alice (heavy solid line) and FAST SANBAR forecast (dashed line). Dots show positions at 24 h intervals. Actual positions are taken from smoothed analysis after the fact. The forecast positions including the initial one, are operational estimates, available in real time. Selected observed winds are indicated in degrees and knots by dddff.

contain an apparent slow bias. Therefore, we believe that a solution of the pervasive slow-bias problem has been attained, though persistent errors for particular storms may be observed.

7. Operational experience in 1973

Thirty-seven FAST SANBAR storm forecasts were made operationally and verified during the 1973 hurricane season. The only gratifying note was that the slow bias had indeed been eliminated. The average first 24 h displacement was 3% fast. Other sources of error, however, were numerous. Beyond the 24 h range, average position errors, shown in Table 1, were larger than those in the 1971 forecasts made by any version of SANBAR, as reported by Pike (1972).

In the 72 h forecasts, accuracy of storm position depends heavily on accuracy in prediction of the large-scale flow patterns. We might suppose that this accuracy would be least where the data are fewest. Indeed, forecasts for Ellen and Alice, storms in the subtropics beyond the reach of the rawinsonde network, suffered large position errors at this range. In Fig. 6 we see an egregiously poor forecast for Alice; the observed storm moves northward at a slowly accelerating rate, while the prediction shows an extremely slow motion, anticyclonically curved. The ridge south of the storm along 20°N developed into a small anticyclone which steered the predicted storm toward the east. In actuality there may well have been a stronger ridge east of the storm with stronger southerly steering flow in its path, and with less cyclonic circulation east of the center than shown in Fig. 6. There are no rawinsonde observations within 600 n mi of the storm except at Bermuda, where the sounding was ignored because of proximity of the storm. Thus the initial analysis depended almost entirely on the bogus data and on the estimated 5 kt initial speed of the storm. In the later portion of this forecast an unpredicted trough development in the eastern United States added to the large-scale southerly flow over the storm, but the error had become established before this time.

An outstanding 72 h forecast failure (for Ellen) is shown in Fig. 7. Only one useful rawinsonde observation (at Bermuda) lies within 1000 n mi of the initial position of the storm. Add to this the inherent uncertainty in a situation when the large-scale flow is markedly diffluent, as it is here, and the failure of the recurvature prediction can be no surprise.

Dramatic errors in the 72 h forecast can also occur

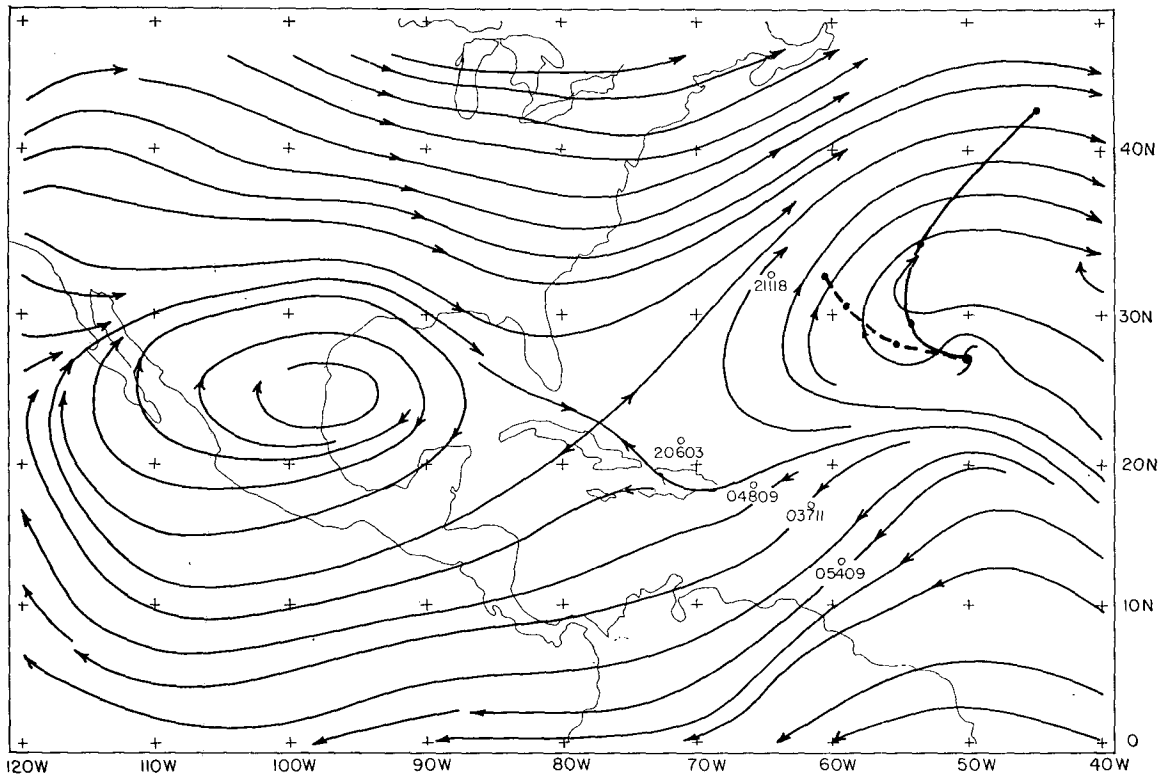

FIG. 7. As in Fig. 6, except at 1200 GMT 19 September 1973, with the tracks of Ellen.

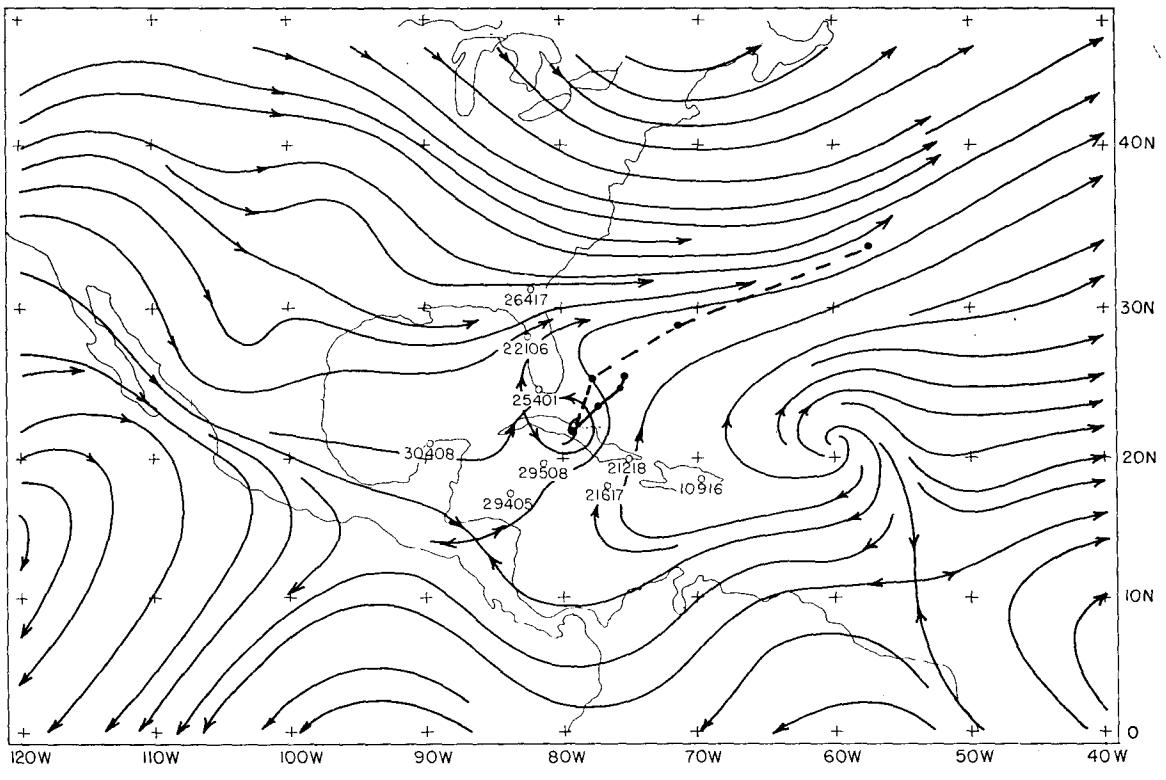

FIG. 8. As in Fig. 6, except for 0000 GMT 19 October 1973, with the tracks of Gilda.

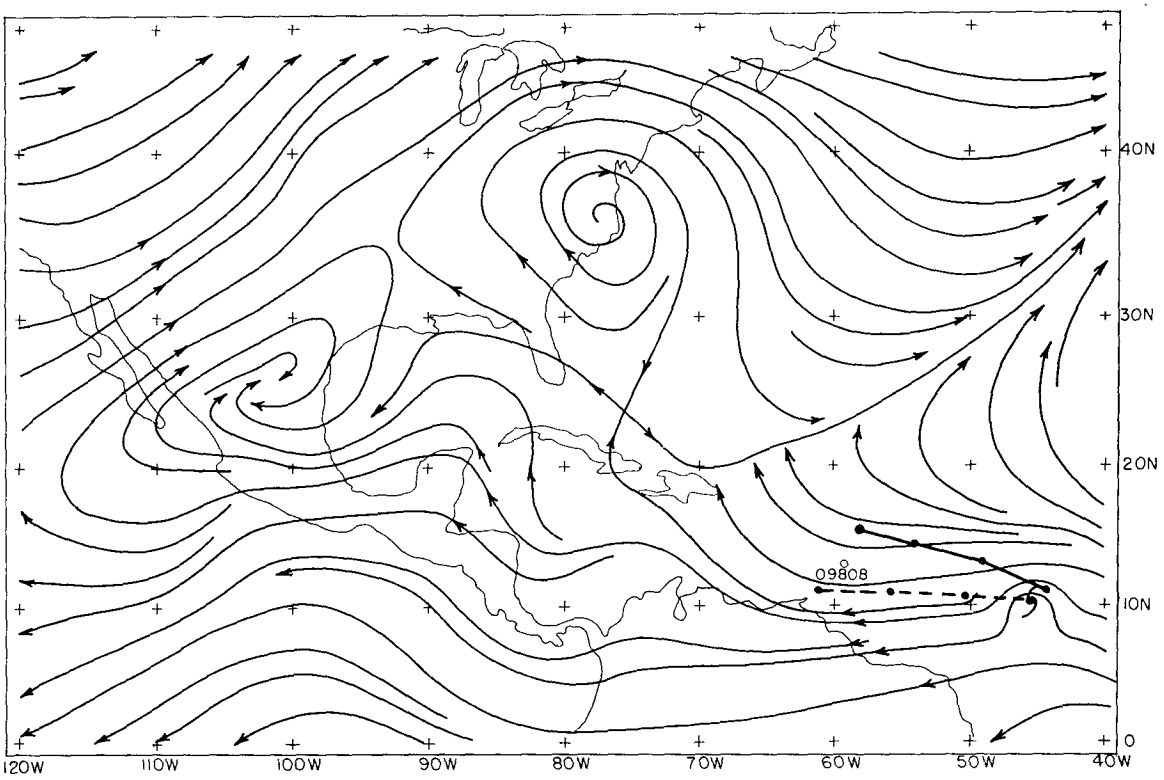

FIG. 9. As in Fig. 6, except at 0000 GMT 31 August 1973, with the tracks of Christine.

in regions of better data coverage. Gilda (Fig. 8) was forecast to accelerate dramatically toward the east-northeast after the first 24 h, whereas in fact it decelerated and became nearly stationary. The 72 h position was in error by 1045 nm. The forecast seems synoptically very reasonable, and even an examination of the actual evolution of the large-scale flow pattern makes it difficult to understand the slowness of the actual path. No observations were available, however, in the northeast quadrant of the storm out to a distance of about 700 n mi. More adequate data coverage might have given a different initial analysis of the large-scale situation.

The 48 and 72 h forecast position errors for Christine were not exceptionally large despite almost complete lack of rawinsondes. This storm occurred in very low latitudes where climatological estimates of both storm motion and environmental flow pattern are relatively accurate.

For the most part, large errors at 24 h range stem from inaccuracy in the estimate of the initial position and velocity of the storm. A large error of this type (for Christine) is shown in Fig. 9. The initial position error of 85 n mi was the largest in this sample of forecasts. There were no data to interfere, in barotropic effect, with linear projection of the estimated initial storm velocity due westward at 15 kt. The storm was later found to be northeast of the estimated position and to be moving toward the west-northwest. The observed track was nearly as steady as the predicted one.

Another example of this kind of problem is given in Fig. 10. Here, in the absence of relevant wind data, the initial estimated storm track velocity toward 275° at 13 kt curved and slowed only slightly during the first 24 h of the forecast, thereafter decelerating dramatically. In the light of hindsight, it was found that Ellen actually had just begun a rather sharp recurvature. Twelve hours later the storm was estimated, even operationally, to be moving toward 330° at 10 kt. This vector discrepancy of about 230° at 11 kt, if viewed as a correction to the 24 h SANBAR forecast, would account for about 260 n mi of the 320 n mi position error. An additional 40 n mi error is attributable to incorrect initial positioning, so it is clear that, with luck, one could obtain an almost perfect forecast with almost no rawinsonde data.

The largest 24 h position error (325 n mi) occurred, however, in a region of plentiful data, as can be seen from Fig. 11. In fact, no less than five soundings were discarded in this instance because they lay in the north and west quadrants of the influence region of Delia. One could hardly imagine a worse forecast at a particularly critical time, 12 h before landfall. The predicted storm moved during the first 12 h with almost the same velocity as the initial specified one:

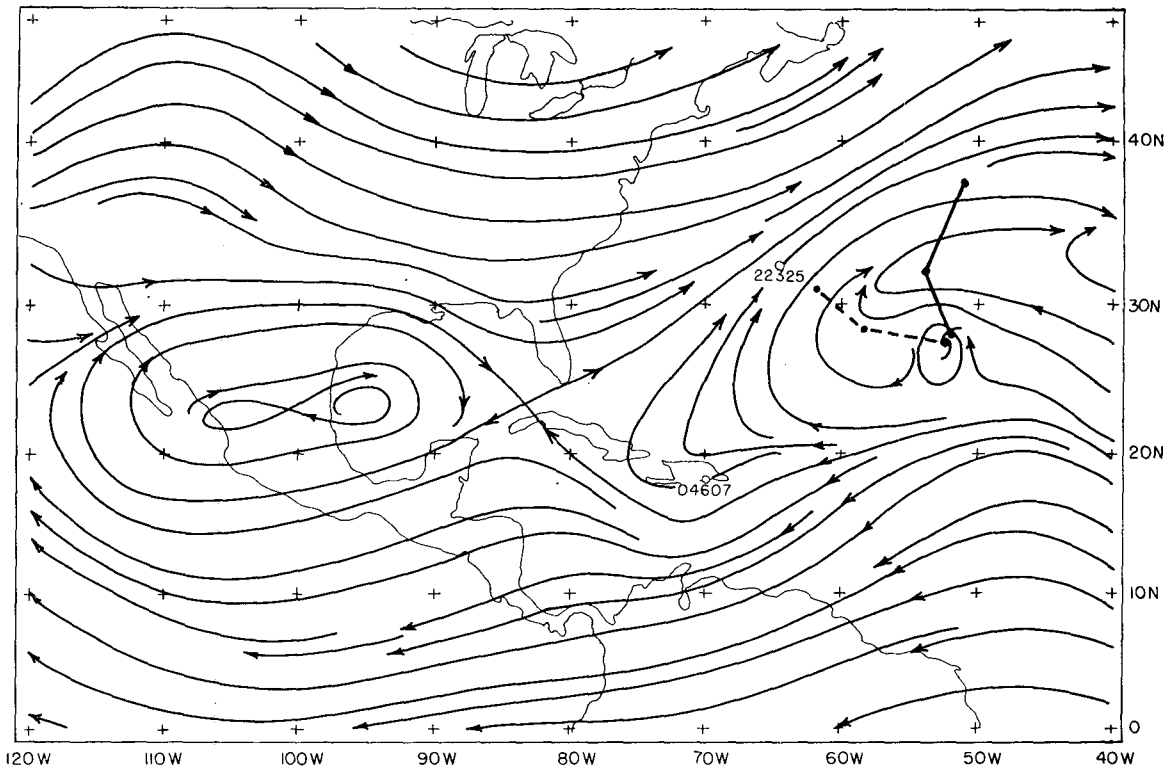

FIG. 10. As in Fig. 6, except at 0000 GMT 20 September 1973, with the tracks of Ellen.

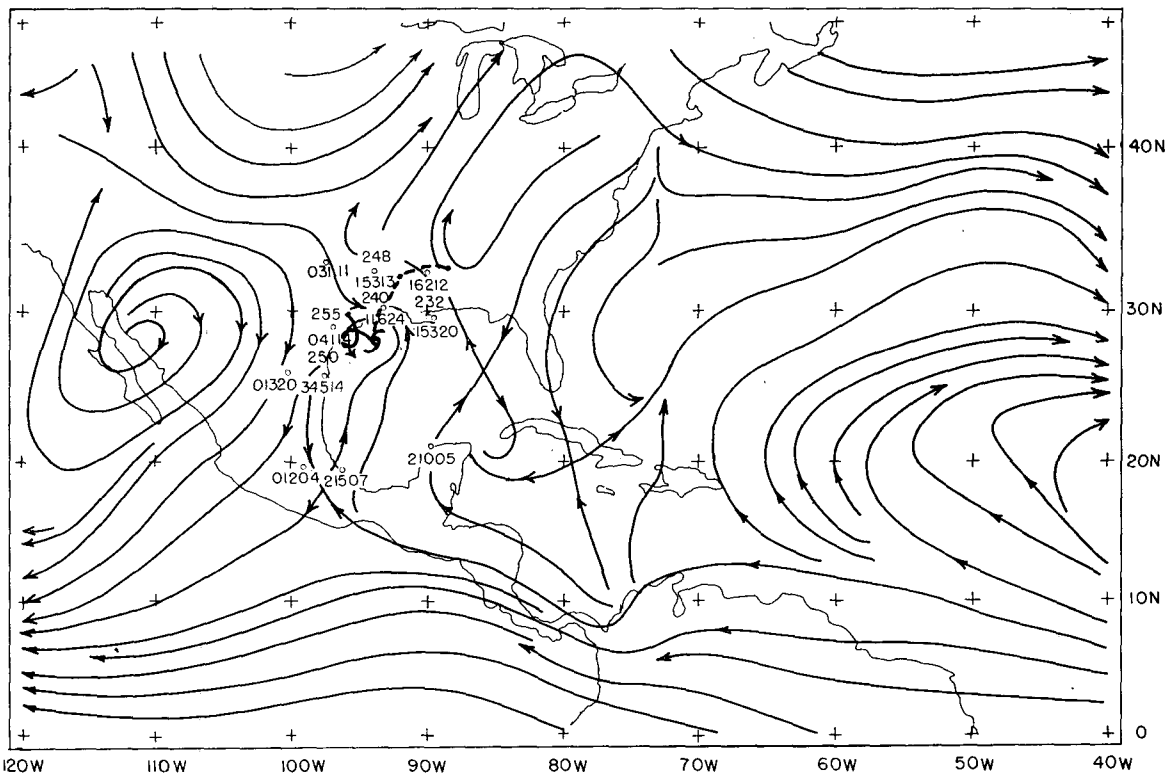

FIG. 11. As in Fig. 6, except at 1200 GMT 4 September 1973, with the tracks of Delia. International index numbers of stations within the initial influence distance of the storm are shown.

TABLE 2. Comparison of observed and replacement winds in vicinity of Delia at 1200 GMT for 4 September.*

Station no.	Observed wind	Replacement wind	Replacement minus observed
232	153/20	170/15	290/07
240	116/24	120/26	170/03
248	153/13	148/14	040/01
250	345/14	182/09	170/23
255	041/14	145/05	245/14
Mean			195/08
Rate of 24 h displacement error			220/13
Initial storm motion			175/12

* All vectors are in degrees and knots.

TABLE 3. Comparison of 24 h SANBAR and persistence displacement errors.*

		Speed		Direction	
Storm	*N*	Persistence error	Mean persistence minus mean SANBAR	Persistence error	Mean persistence minus mean SANBAR
Alice	6	3.3	+0.8	7.5	−1.3
Brenda	4	1.8	+0.5	29.8	+0.2
Christine	6	2.3	+0.8	10.5	−3.2
Delia	6**	5.0	+1.2	47.0	−5.2
Ellen	6	3.5	+2.0	30.2	+10.3
Fran	1	7.0	+2.0	3.0	−4.0
Gilda	8	2.0	−1.4	27.1	+5.8
All storms	37**	3.1	+0.6	24.0	+1.4

* Persistence errors are average magnitudes of errors for each storm and for the entire sample. "Mean persistence minus mean SANBAR" is the algebraic difference of mean magnitudes for each storm and for the entire sample. Errors are in degrees and knots.
** Direction errors were evaluated for only five Delia forecasts, since one persistence value was zero motion.

toward 355° at 12 kt. Then it recurved inland toward the east and decelerated. The actual storm moved northwestward at 11 kt for the first 12 h, grazed the coast, then slowed suddenly, moved in a counterclockwise circle with radius about 30 n mi, and made a second landfall a short distance southwest of the first one, crossing the coast about 66 h after initial time and moving inland in southeast Texas.

Errors in initial positioning and storm velocity were damaging in this case. The operational estimates 12 h earlier and later were toward 298° at 15 kt and toward 304° at 7 kt, respectively. It is not clear what abberation in the data prompted the operational estimate at 1200 GMT 4 September.

Probably more important, though, was the treatment of the wind data along the Louisiana and Texas Gulf coasts. The discarded observations and their manufactured replacements are given in Table 2. Note that the vector differences from the observed winds to the replacement values are generally in the same direction as the error in the 24 h forecast. There is no guarantee, however, that a return to the original SANBAR model in cases like this one would provide good forecasts. A forecast made (after the fact) with the original SANBAR model, yielded a much improved track for the initial data shown in Fig. 11. The first point of landfall was predicted almost exactly correctly, and the 24 h position error was an acceptable 85 n mi. The loop offshore was not predicted, however. Williams (1972), moreover, discusses an example (for Fern at 1200 GMT 9 September 1971) which is remarkably similar to this Delia case with respect to initial location, actual track, and forecast error. In the Fern case the subtraction of the idealized storm component, as in the original SANBAR model, left an unrealistic steering component which the predicted storm tended to follow. We do not appear, then, to have a satisfactory way of taking account of wind observations within the region influenced by the storm.

Despite all these shortcomings, the forecasts as a group appeared to show modest skill. Skill is here defined as incremental accuracy beyond what is attained by application of some simple control forecast. SANBAR performance at 24 h range in comparison to persistence of the operationally determined initial storm direction and speed is given in Table 3. Little significance can be attached to the small improvement in direction since there was an average loss to persistence in four of the seven storms, and since the net gain was a miniscule portion of the average persistence error. The improvement in speed, however, appears to be more meaningful since it represents about 20% of the average persistence speed error, and since improvement was shown for all storms except Gilda.

We believe that FAST SANBAR has skill at all ranges, even in comparison with such sophisticated combinations of persistence and climatology as the HURRAN (Hope and Neumann, 1970) and CLIPER (Neumann, 1972) forecasts. This assertion, however, bears a close resemblance to a testament of faith, since operational results to date are few and ambiguous. Such results in 1973 are given in Table 4, in which we see that the SANBAR results are inferior to the CLIPER forecasts at ranges of 48 and 72 h.

TABLE 4. Comparative position errors (n mi) of 1973 SANBAR forecasts and concurrent HURRAN and CLIPER forecasts.

	Time range		
	24 hours	48 hours	72 hours
N	28	20	9
SANBAR	106	305	407
HURRAN	127	325	418
N	37	25	12
SANBAR	103	295	480
CLIPER	115	278	363

Note: It is not possible to present a large homogeneous set of results because of the frequency with which one or another of the forecast methods did not yield a prediction, for one reason or another, and because of the lack of verifying positions which arose from a variety of considerations (see Table 1).

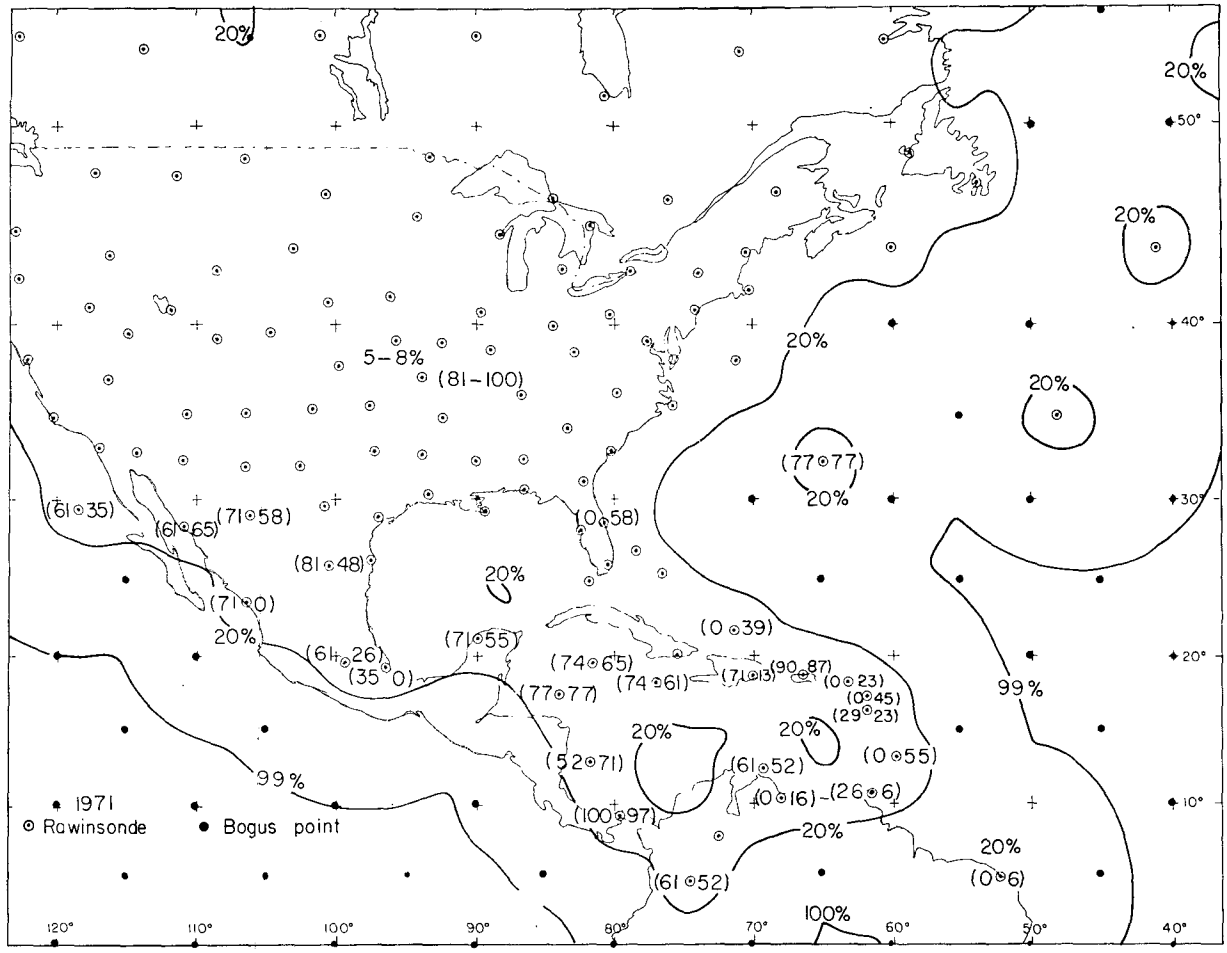

FIG. 12. Map of unexplained variance in the analysis of the deviation of the zonal wind component from its zonal mean, given rawinsonde observations at locations shown by the circled dots. Only the 20% and the 99% lines are shown. Numbers within parentheses at selected stations are percentages of possible observations in a recent month available in useful form at the National Meteorological Center for 0000 GMT at the left and 1200 GMT to the right of the station circle (Finger and Thomas, 1973).

This comparison was strongly influenced by the (we hope) extraordinarily large errors encountered in SANBAR forecasts for Gilda and Ellen of which Fig. 8 gives an example. Our optimism relies on the 1971 results given by Pike (1972) and the 24 h results for 1973.

8. Improvement in accuracy of track forecasts

In the search for improved accuracy in prediction of the tracks of tropical storms, one naturally considers the development of a physically more sophisticated model. In the prediction of intensity, such a model is undoubtedly desirable; the intensity in the SANBAR forecast is nearly constant in principle and is eroded by truncation error in practice. So far as motion is concerned, there is no reason to doubt that asymmetries of mechanical or thermodynamic origin which would appear only in a baroclinic model can have an effect on the track of the storm. We take the position that these effects are secondary, that the primary effect is gross vorticity advection, and that uncertainty in the measurement of this advection now primarily limits the forecast accuracy.

In improving the performance of this model we face two complementary difficulties: if rawinsonde data are present within the influence region of the storm we now find it regretably necessary to discard them; and if no such data are present within the storm region or a few hundred miles beyond, our portrayal of even the larger synoptic-scale features is uncertain.

This latter difficulty is underlined by the information shown in Fig. 12. Here we see the residual uncertainty in the analysis of the zonal wind, given data from all the rawinsonde locations shown. (This map is a by-product of the calculation of regression equations for the grid points from the September 1971 data sample, as explained earlier.) It is evident that

much tropical storm activity takes place in regions where this uncertainty is greater than 20%.

Even this picture is optimistic, for the observational coverage is never complete. It is clear that a number of stations are scheduled to make observations at either 0000 or 12000 GMT but not both, and that reception is woefully incomplete for some stations even when observations are scheduled. Since the Ocean Weather Stations have been discontinued at 35°N, 49°W and at 44°N, 41°W, and since the reception of an observation from the station at 5°N, 52°W is a rare event, the Atlantic Ocean south of 40°N and east of 50°W is an abyss of total ignorance so far as rawinsonde data are concerned.

Our national interests are not immediately and strongly affected by storms in this area so far at sea, of course, but it is significant that there is an additional maximum of unexplained variance in the Gulf of Mexico, a region from which only one storm in history has failed to make landfall either (most likely) in the United States or in Mexico or Cuba. The analysis in the Gulf, moreover, relies heavily on the observation from Merida at 21°N, 90°W. Should this observation be missing, the uncertainty of the analysis in the central Gulf rises to about 50%. The stationing of a weather ship in this area during the hurricane season would improve matters considerably.

In the other regions of sparse data it is clear that reliance must be placed on observations from aircraft, from ships, and from satellites. Studies of optimum ways to combine these data, so as to replicate the tropospheric mean wind as given by rawinsonde, are being undertaken at the National Hurricane Center (NHC).

The opposite problem should also be dealt with, since the data now being discarded must be potentially valuable. The theoretical profile for the storm wind is given by

$$|V| = 0.72 V_{\max} \left\{ \sin\left[\pi \left(\frac{R}{R_{\max}} \right)^{\log 0.5 / \log (R_{\text{eye}}/R_{\max})} \right] \right\}^{1.5} \quad (8)$$

where $V_{\max}$ is understood to be the maximum wind, say, as given in the current hurricane advisory, R the distance from the center of the storm to the point in question, R_{eye} the distance from the center to the maximum wind (taken as equal to the eye diameter, usually 20 n mi), and $R_{\max}$ the maximum influence distance of the storm. The factor 0.72 was chosen only because it was the ratio between the boundary-layer maximum wind and the tropospheric mean in the comprehensive profile for Hilda 1964 given by Hawkins and Rubsam (1968). The power 1.5 was chosen empirically after a period of experimentation described by Sanders (1970), but is not sacrosanct. Estimates from surface maps, as discussed above, are the source of values of $R_{\max}$. It would seem that there is plenty of room for accommodating the profile to a number of wind observations in the vicinity. Optimum ways of doing this should be studied without delay.

If progress is made with these reasonably straightforward problems, we estimate that we should be able to reduce position errors for an average sample of all types of tropical storm in all geographical locations and synoptic circumstances to about 75 n mi, 150 n mi and 300 n mi at ranges of 24 h, 48 h and 72 h, respectively. These forecasts should show substantial skill with respect to persistence and climatology at all ranges. The sparsity of tropical storms in the NHC area of responsibility, and the diversity of their behavior, indicate that we shall have to wait a number of years to be confident that such a level of accuracy has in fact been reached. (The waiting period might be shorter if skill rather than accuracy were the measure.) Serious consideration might be given to simply adapting the model to the more fruitful test bed in the western North Pacific Ocean.

9. Concluding comments

We have developed a barotropic model specifically designed for prediction of the track of a tropical cyclone. The model in its present version appears to demonstrate small positive skill with reference to climatology and persistence at ranges from one to three days in advance. Present limitation on forecast accuracy is lack of rawinsonde data in the Atlantic Ocean and inability to make consistently good use of information contained in soundings made within the region influenced by the storm. We suggest means of dealing with these limitations. The 24 h error would then be almost entirely due to erratic day-to-day or hour-to-hour motion of the storm about its longer term smooth trajectory. At 72 h this error source would be joined by a substantial additional error due to inadequacy in prediction of the large-scale aspects of the flow pattern. Baroclinic models will be needed to reduce both these sources of error but will probably require substantially more and better data than now seems in prospect.

Acknowledgments. Among the many whom the authors wish to thank for their contributions to the development of the model, we wish to express particular appreciation to Dr. Peter P. Chase, NOAA, for his construction of the very adroit and effective analysis program. The work has been supported by NOAA National Hurricane Research Laboratory under Grants WB-62, E22-77-67(G), E22-37-71(G) and 04-3-022-7.

REFERENCES

Bowie, E. H., 1922: Formation and movement of West Indian hurricanes. *Mon. Wea. Rev.*, **50**, 173–179.

Cressman, G. P., 1958: Barotropic divergence and very long waves. *Mon. Wea. Rev.*, **86**, 293–297.

Eddy, A., 1967: The statistical objective analysis of scalar data fields. *J. Appl. Meteor.*, **6**, 597–609.

Finger, F. G., and A. R. Thomas, 1973: Toward developing a quality control system for rawinsonde reports. NOAA Tech. Memo. NWS NMC-52.

Gaertner, J. P., 1973: Investigation of forecast errors of the SANBAR hurricane track model. S.M. thesis, Dept. of Meteorology, MIT.

Gandin, L. S., 1963: *Objective Analysis of Meteorological Fields*. Leningrad, Gidrometeor. (Jerusalem, Israel Program for Scientific Translations, 1965.)

Hawkins, H. F., and D. T. Rubsam, 1968: Hurricane Hilda, 1964: II. Structure and budgets of the hurricane on 1 October 1964. *Mon. Wea. Rev.*, **96**, 617–636.

Hope, J. R., and C. J. Neumann, 1970: An operational technique for relating the movement of existing tropical cyclones to past tracks. *Mon. Wea. Rev.*, **98**, 925–933.

Jordan, E. S., 1952: An observational study of the upper-wind circulation around tropical storms. *J. Meteor.*, **9**, 340–346.

Neumann, C. J., 1972: An alternate to the HURRAN tropical cyclone forecasting system. NOAA Tech. Memo. NWS SR-62.

Pike, A. C., 1972: Improved barotropic hurricane track prediction by adjustment of the initial wind field. NOAA Tech. Memo. NWS SR-66.

Phillips, N. A., 1972: Class notes. Dept. of Meteorology, MIT.

Sanders, F. 1970: Dynamic forecasting of tropical storm tracks. *Trans. N. Y. Acad. Sci.*, Ser. II, **32**, 495–508.

——, and R. W. Burpee, 1968: Experiments in barotropic hurricane track forecasting. *J. Appl. Meteor.*, **7**, 313–323.

Shuman, F. G., and L. W. Vanderman, 1968: Operational methods of truncation error control. *Lectures on Short-Range Weather Prediction*, Leningrad, Hydrometeoizdat, 178–187.

Williams, F. R., 1972: Application of the SANBAR hurricane track forecast model. S.M. thesis, Dept. of Meteorology, MIT.